Textures and Microstructures, 1991, Vols 14–18, pp. 953–958
Reprints available from the publisher
Photocopying permitted by license only

DISLOCATION MICROSTRUCTURES AND TWINNING INITIATION IN CU-AL ALPHA FCC SINGLE CRYSTALS: EXPERIMENTAL AND NUMERICAL ANALYSES

P. FRANCIOSI[1], F. TRANCHANT[2], J. VERGNOL[2]

[1]Laboratoire PMTM UPR9001 CNRS, Univ. Paris Nord, Villetaneuse France
[2]Laboratoire de Métallurgie Physique, URA131 CNRS, Univ. Poitiers France

ABSTRACT

The dislocation structures at the onset of twinning for <111> tension tests on variously prestrained FCC single crystals are experimentaly and numericaly analyzed to investigate twinning initiation conditions and discuss the appropriate criterion expression.

KEYWORDS

Single crystals, dislocation microstructures, twinning initiation

INTRODUCTION

For a better understanding of twinning initiation mechanisms in strained single crystals, still not accounted in plasticity codes for aggregates, experimental observations on FCC Cu-Al alpha samples and numerical simulations are compared at the dislocation density scale. Both experimental and numerical tests consist in a $|\bar{3}12|$ compressive prestrain to various amplitudes, followed by an uniaxial tension along the $|111|$ transversal axis. According to the evaluated dislocation patterns in the different situations from both TEM observations and numerical simulations, twinning initiation mechanisms and criteria are discussed.

EXPERIMENTAL RESULTS

All experiments have been performed at room temperature on samples with 7.3 at Al. Two serie of samples have been prestrained up to (1) 3.5 and (2) to 8.6 per cent compression respectively. For the first series, TEM observations reveal, after the compressive prestrain, a dominant density of primary dislocations on the $(\bar{1}\bar{1}1)$ $|1\bar{1}0|$ system - C5 in the Schmid and Boas convention - while in the second series, numerous Lomer Cottrell (LC) locks, mainly of the $|\bar{1}01|$ Burgers vector and lying along the $|101|$ orientation, (here denoted 3/4), are observed.

A perfect uniaxial tensile test along a <111> axis would equally stress 6 slip systems. On the experimental σ/ε stress strain curves (fig. 1), the slipping stage prior to the twinning initiation corresponds, for unprestrained samples, to an observed dominant slip on the A and D planes. TEM observations do not reveal Lomer dislocations which would be present if conjugate system pairs were active simultaneously. A two orientations walls microstructure has developed (fig. 2).

After prestrain, the C slip plane is in both cases the first active one in tension (fig. 3). At small tensile deformation, the C1 system dominant activation is supported by the TEM observation of LC 3/4 locks (fig. 4), the density of which increases with strain (fig. 5), and which can only result from C1-A6 interactions during such a <111> tensile test. If for the samples (1), all the LC 3/4 are created during the <111> secondary tension test, for the samples (2) they both come from the prestrain and from further multiplication during the subsequent tension. The slope changes on the σ/ε curves (fig. 2) generally correspond with modifications of the relative slip plane activity. After the C plane activation, the microscopic observations reveal a high activity on the A plane, and a significant density of LC 2/1 which supports some activity on the "unexpected" B plane (fig. 6).

These experiments indicate that the modification of the as grown dislocation network firstly acts on the slip mode which initialy ensures the tensile deformation, and consequently on the microstructure from which twins initiate and grow (1). Three different situations arise:
- without any prestrain, twinning occurs on the less active plane during the previous slip stage of the tension test (i-e here the C plane),
- after the small compressive prestrain, twinning in <111> tension initiates at a larger stress and develops on the A and C planes, with a dominant activity on A,
- after the large prestrain, twinning occurs on the C plane, say one of the most active planes during the previous slipping stage of the tension test, at a stress comparable to the one of the unprestrained case.

The figure 10 reports the twinning stress during tension, with the active mode changes, as a function of the prestrain amplitude. One must stress the fact that the increasing C twin system activity with increasing prestrain cannot here be justified by pure lattice rotation effects.

NUMERICAL SIMULATIONS

The here used code for FCC single crystal plasticity is based on a microstructural hardening law previously introduced (2) which typically expresses the critical shear stress rates on any g system as a function of the density evolutions on the various cristallographic ℓ systems of the structure. It allows to estimate the glissile and sessile dislocation interaction products as long as the plastic deformation is performed by slip. Written in a finite elastic plastic deformation formalism previously developed in (3), this code is governed by the prescription of mixed and regular conditions in conjugate stress and strain rates, under the assumption of an uniform response of the single crystal.

The $|\bar{3}12|$ compression test simulation, which will be presented in a forthcoming extended paper, is consistent with the stage one primary C5 system activity and the dominant LC 3/4 locks multiplication in the stress strain curve stage two. The simulated <111> σ/ε curves are reported figure 8 for the unprestrained case and for three different prestrain amplitudes, respectively in stage one (I), at the stage transition (I'), and in stage two (II). The related slip activities are plotted respectively on figure 7,a,b,c,d and the corresponding evolutions of the main LC lock densities are gathered on the figure 9.

These results qualitatively predict the main experimental features except for the unprestrained tension which keeps the ternary symetry of the <111> axis and predicts activity of the three A,C,D planes. However, only three systems, alternatively (A6,C3,D1) and (A3,C1,D6), appear

simultaneously active and without conjugate pairs, what minimizes the LC locks multiplication as observed. After prestrain, the C1 system is the initialy dominant one due to anisotropic hardening, the A6 further contribution increasing with the prestrain amplitude. The LC 3/4 locks density is or remains the dominant one, due to C1-A6 interaction. The singularity on the simulated σ/ε curves for the prestrained samples correspond, as observed, to the momentary activity of the B plane, responsible for extra LC locks creations such as the 2/1 type ones.

Since the code does not account for mechanical twinning, the subsequent simulated behaviour is not to be compared with the experiments. However, expecting the onset of twinning to follow the B plane activity, a particular attention has been paid to the evolution of the cristallographic and microstructural parameters up to this "critical" stage.

The evolution of the applied resolved shear stress (ARSS) on the 3 twinning systems concerned with a <111> tension is reported on figure 11 versus the tensile stress. The intersection of these $\tau tw/\sigma$ curves with a critical twinning shear stress $\tau ctw=cst$ (dotted) line, at tensile stresses above the B slipping threshold, defines a critical twinning stress σtw, which is in turn plotted as a function of the prestrain amplitude (fig 11b). This $\sigma tw/\varepsilon$ curve does not fit the experimental one. According to Fontaine analysis (4), developed by Vergnol et al (5) for low stacking fault energy solid solutions, a twinning initiation criterion of the form:

$$N.\tau_{tw} = \tau_{ctw},$$

where N is an average pile up size on glide obstacles, has been defined using for N, the Cohen and Weertman description (6) of the twinning initiation process at the dislocation scale in the FCC structure: the mobile dislocations of an active slip system in a P octahedral plane pile up on obstacles of the Lomer Cottrell lock type, lying at the intersection of two octahedral P and P' planes. At a large enough shear stress these piled up dislocations dissociate so as to emit in the P' plane partial dislocations which "drag" microtwins. Piling up of C1 (resp A6) dislocations on LC 3/4 would therefore lead to A (resp C) twinning.

We have here roughly defined the N pile up size for a given active slip system as the ratio of the mobile dislocation density on the active system to the square root of the corresponding Lomer Cottrell locks density, a debatable definition which cannot be valid when the obstacle density is weak. These $N.\tau tw$ versus σ simulated curves are reported on the figure 12, and the corresponding critical twinning stress evolution with the prestrain amplitude (defined as in figure 11, by the intersection with a line $\tau ctw=cst$ at a large enough stress) is plotted figure 12b. With such a criterion, the preferred twinning on plane A at small prestrain and on plane C at larger one are correctly predicted but not the critical twinning stress variation with the prestrain.

A third criterion, of the form $N.\tau = \tau_{ctw}$,

where the ARSS τ on the slip system of which the dislocations pile up on the obstacles replaces the ARSS on the corresponding twinning system, has been considered. The figure 13 a and b show the simulated $N.\tau$ versus σ curves so obtained and the related $\sigma tw/\varepsilon$ curve still defined for a constant twinning threshold. This curve fits the experimental one (fig 7) with respect to both the preferred twinning plane and the evolution of the critical twinning stress with the prestrain amplitude.

CONCLUSION

From the comparison between observations and numerical simulations, the twinning modes and the twinning stress do not appear correctly predicted with only the macroscopic assumption of a constant critical shear stress on the twinning systems. A better fit is here obtained accounting for local stress conditions ahead of mobile dislocation pile ups from which twin can initiate according to a mechanism involving the Lomer Cottrell locks, even with a rough estimate of these pile up size.

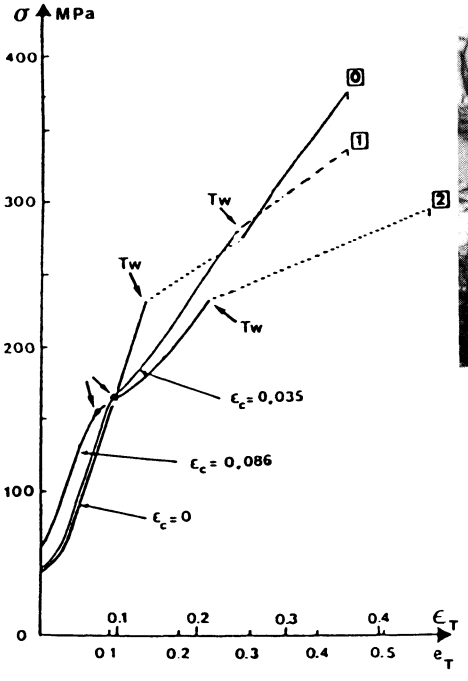

Figure 1: tensile σ/ε curves for virgin and serie 1 and 2 crystals.

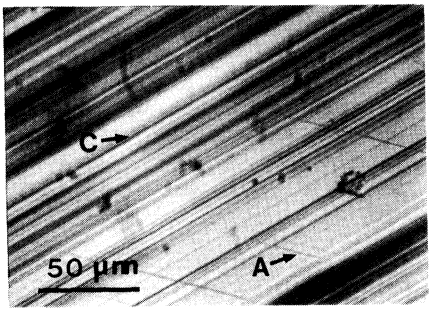

Figure 3: slip on C plane for a series 1 crystal at ϵ_T=0.03.

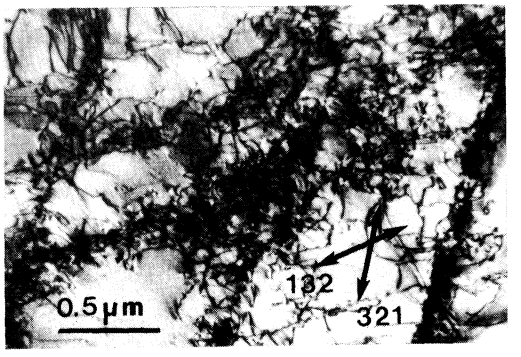

Figure 2: dislocation walls in a virgin crystal (ϵ_c=0) strained in tension (ϵ_T=0.1).

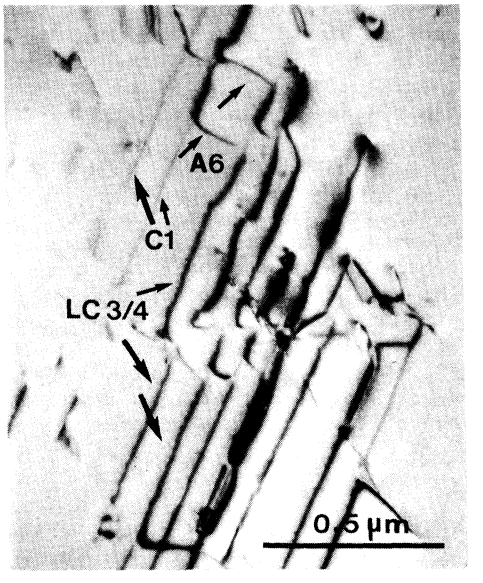

Figure 4: first arrays of LC 3/4 locks for a series 1 crystal at ϵ_T=0.03

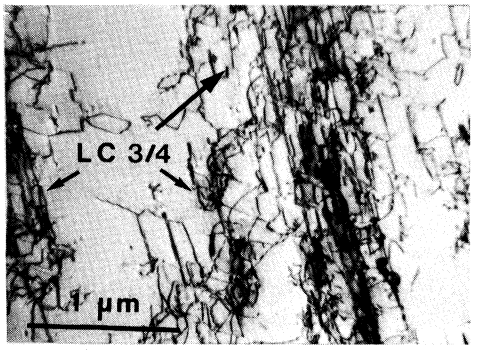

Figure 5: high deformation LC 3/4 arrays (series 1 sample, ε_T=0.15)

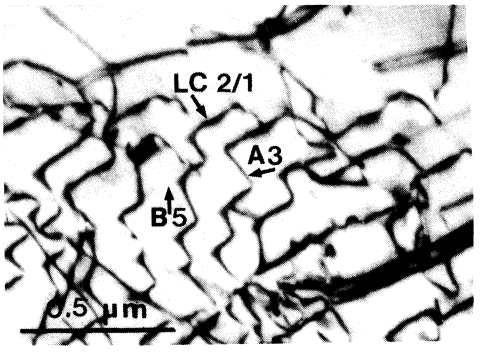

Figure 6: network of LC 2/I locks (series 1 sample, ε_T=0.15)

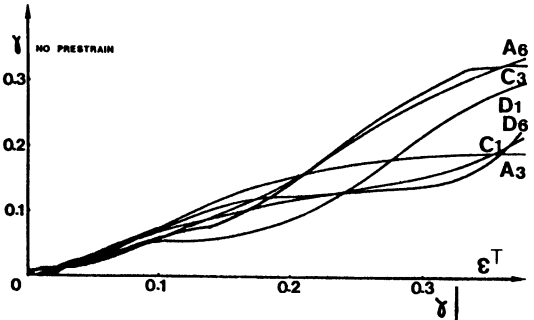

Figure 7: slip vs strain on the active systems for each a(unprestrained), b(I), c(I'), d(II) tensile tests simulation

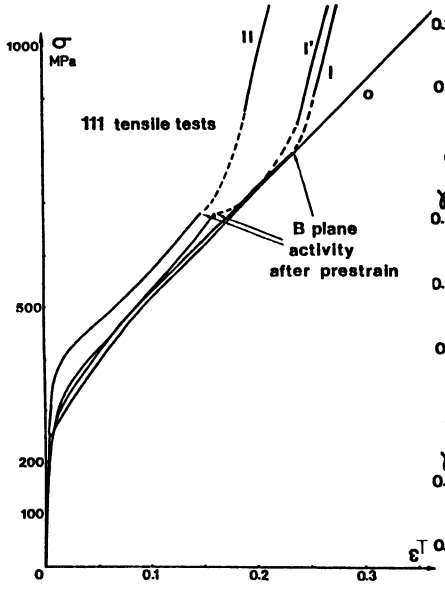

Figure 8: simulated tensile σ/ε curves for various prestrain amplitudes

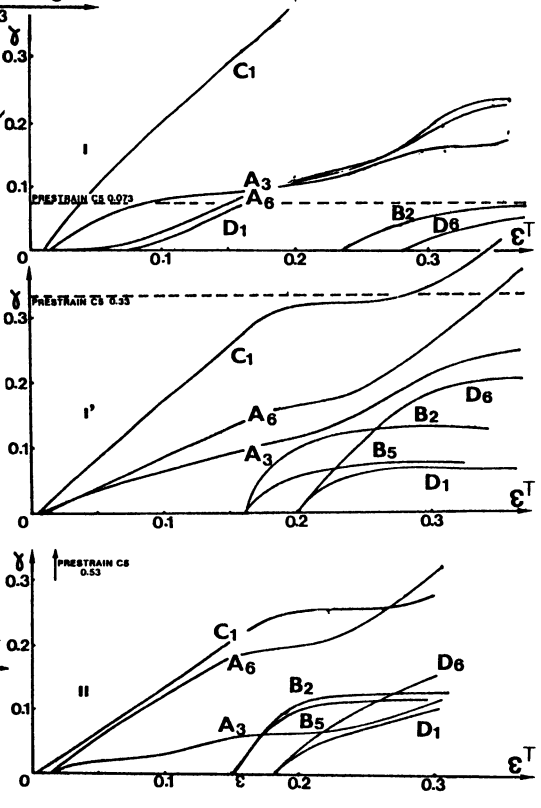

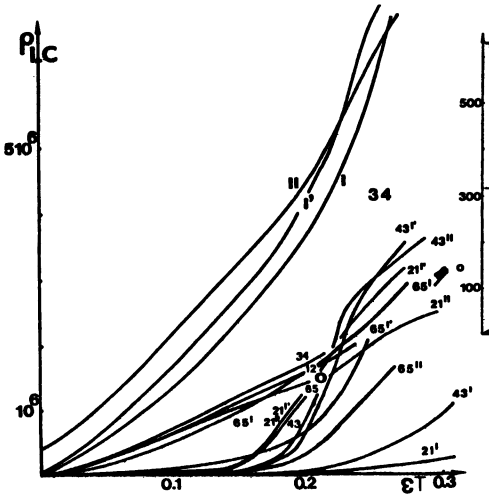

Figure 9: the LC locks main density evolutions with strain in simulated tension for the various prestrained cases

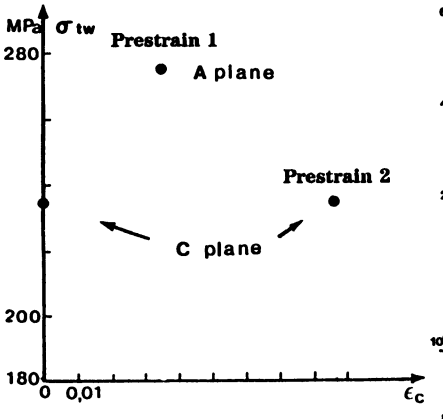

Figure 10: experimental twinning stress vs prestrain amplitude ε_c and twinning planes

Figure 13: the twinning stress vs εc curve (b) from a modulated ARSS on the slipping systems (a)

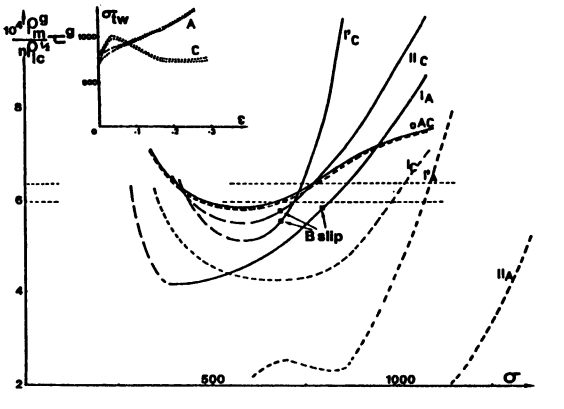

Figure 11: the ARSS on the twinning systems vs tensile stress for each simulated case (a) and the related twinning stress vs ε_c (b) curves

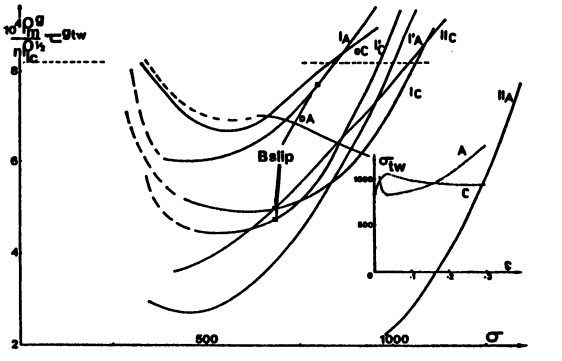

Figure 12: the twinning stress vs εc curve (b) from a modulated ARSS on the twinning systems (a)

REFERENCES

1. F.Tranchant, Doctorate Thesis, Poitiers, France (1987)
2. P. Franciosi, Proceedings of the 8th RISO Conf, 87, (1988)
3. P. Franciosi and A. Zaoui, Int. J. Plasticity, to be published
4. G. fontaine, Doctorate Thesis, Orsay, France (1968)
5. J.Vergnol, J. Grilhé, J. Physics, 45, (1979)
6. T.B. Cohen, J. Weertman, Acta Metall, 11, 996, (1963)